Ab Initio and Density Functional Study of the Conformational Space of $^{1}C_{4}$ α-L-Fucose

GÁBOR I. CSONKA* and KRISZTINA ÉLIÁS

Department of Inorganic Chemistry, Technical University of Budapest, H-1521 Budapest, Hungary

IMRE G. CSIZMADIA

Department of Chemistry, University of Toronto, Toronto, Ontario M5S 1A1, Canada

ABSTRACT

The conformational space of $^{1}C_{4}$ α-L-fucose was searched by the MM2*-SUMM molecular mechanics conformational search technique. The molecular geometries of the first 17 structures of lowest energy were analyzed at the HF/3−21G, 6−31G(*d*), and generalized gradient approximation (GGA) DFT levels of theory. © 1997 by John Wiley & Sons, Inc.

Introduction

The orientations of carbonhydrate hydroxyls affect the reactivity of sugars in glycosylation reactions.[1,2] The reliable prediction of the orientations of these hydroxyl groups would greatly help investigators and would lead to a better understanding of the molecular recognition of sugar molecules (e.g., in cell adhesion, metastasis, fertilization, or embryonic development), and carbohydrate-receptor binding.[3,5] The numerous inter- and intramolecular OH ··· O interactions in sugars and polysaccharides make these analyses extremely complicated. According to multidimensional conformational analysis, the threefold rotation of *n* hydroxyl groups, in principle, can generate 3^{n} different conformers. The α and β anomers and aldopyranosyl ring puckering (two nonequivalent, chairlike $^{4}C_{1}$ and $^{1}C_{4}$,[6] skew and skew-boat forms[7] should also be considered) leads to additional structures. This complexity makes the sugars and oligosaccharides excellent information encoders that may be decoded by a given receptor during the biomolecular binding process. This process is entropically unfavorable due to the decrease of rotational and translational entropy.[8-10] To estimate the magnitude of this entropy decrease, the entropy of the unbinded carbohydrates would be known.

The conformation of carbohydrates in solution can be established by the combination of NMR

---

*Author to whom all correspondence should be addressed.

spectroscopy and molecular mechanics and dynamics techniques.[11] However, there are serious problems with the force-field calculations that arise from the insufficient quality parameter sets for saccharides.[12] The comprehensive, high-quality *ab initio* calculations may help to point out the problems with the force fields.

The L-fucose group is an important building block of polysaccharides.[13] It has a sufficiently simple structure; consequently, its hydroxyl interactions can be studied at a rather high level of theory. The conformational space for $^1C_4$ α-L-fucose is shown in Figure 1. Note that only the carbon atoms are numbered. These same numbers will be used to denote the oxygen atoms attached to those carbons throughout this article. Following conventional notation, the idealized dihedral angles are designated by g+, t, and g− for *gauche* clockwise (60°), *anti* (180°), and *gauche* counterclockwise (−60°), respectively, for the C—C—O—H torsions. It should be noted that the *anti* position is denoted by the letter ''t'' and not by the letter ''a,'' because the latter is reserved for the notation of the axial positions of hydroxyls in sugars.

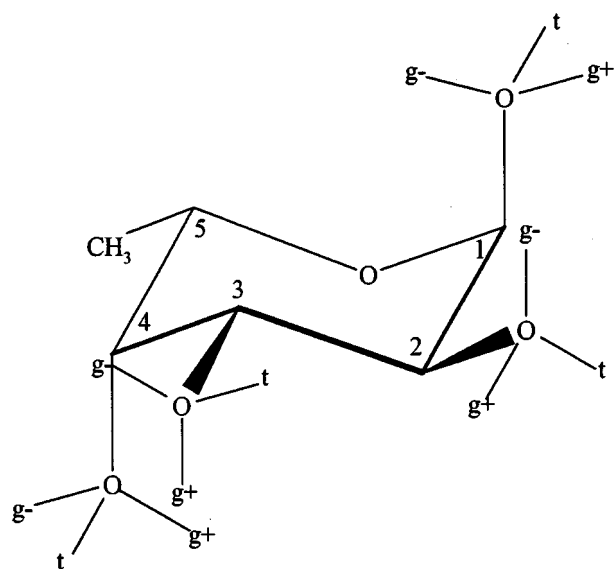For aldopyranohexoses, the threefold rotational of the five hydroxyl groups and the C—C bond of the hydroxymethyl group, in principle, can gener-ate 729 different conformers[14, 15] for a given anomer and chair form. Our previous study showed that the OH···O interaction between one of the ring hydroxyl groups and the hydroxymethyl group differs considerably from the three interactions between the four ring hydroxyl groups.[15] Moreover, the hydroxymethyl group rotates more freely than the ring hydroxyl groups.[15] In α-L-fucose, the lack of a hydroxymethyl group considerably reduces the possible number of minima on the potential energy hypersurface (PEH). The remaining four hydroxyl groups provide 81 possible minima on the PEH (cf. Fig. 1).

A proton NMR investigation of 23 monosaccharides[16] showed that intramolecular OH···O interactions influence the chemical shifts in sugar anions and explains the differences between the pK values of the anomeric hydroxyl groups. Also, NMR signals of the equatorial hydroxyls are influenced by the equatorial or axial positions of their neighbors. A semiquantitative description of the torsions of the H—C—O—H bonds was also attempted using the vicinal and long-range coupling constants.[16] The smaller magnitude of the vicinal coupling constants of the axial hydroxyls was attributed to an assumed gauche H—C—O—H dihedral angle (±44°). The larger vicinal coupling constants of the equatorial hydroxyls were attributed to partially *anti* H—C—O—H dihedral angles. For α-D,L-fucose, the H—C1—O—H and H—C4—O—H dihedral angles were assumed to be +44° and −45°, respectively.[16]

In the present article, the conformational space of $^1C_4$ α-L-fucose is searched by the MM2*-SUMM method.[17] We analyzed the first 17 low-energy structures at the MM2,[18] AM1[19], PM3[20], HF/3−21G, 6−31G(d), and generalized gradient approximation (GGA) DFT levels of theory. We are looking for the lowest level of the theory that provides chemically useful accuracy. We will compare the results of the present study to the results obtained by high-level methods for 1,2-ethanediol.[21] The predicted dihedral angles can be directly compared to the proton NMR results.[16]

FIGURE 1. Schematic representation of 81 possible minimum energy rotamers of $^1C_4$ α-L-fucose. The idealized C(x + 1) −Cx — O — H torsions are denoted by g+, t, and g−for *gauche* clockwise (60°), *anti* (180°), and *gauche* counterclockwise (−60°), respectively, where x = 1, 2, 3, 4.

Computational Methods

The search for stable rotamers in the conformational space of $^1C_4$ α-L-fucose was carried out using the MacroModel 4.5 program package.[22] The MM2* force field available in MacroModel has been used. It differs from the original MM2 force

field[18] only in that it employs the point-charge Coulomb potential to describe the electronic electrostatic interactions. The conformational space was searched using a particularly efficient systematic unbounded multiple minimum search technique (SUMM)[17] that is available in MacroModel. The resulting 415 rotamers were minimized to yield 17 unique rotamers within an energy window of 40 kJ/mol above the global minimum. Geometry optimizations were carried out with a truncated Newton conjugate gradient (TNCG) technique[23] with the maximal number of iterations set to 200 and using a convergence criterion of 0.01 for the gradient norm. The global minimum was found 39 times.

The 17 minima obtained by the MM2*-SUMM search were further optimized by AM1, PM3, HF, and generalized gradient approximation (GGA) and hybrid density functional (DFT) methods using the Berny algorithm combined with redundant internal coordinates built into the GAUSSIAN 94 program.[24]

We employed the following combinations of the GGA−DFT functionals:

1. The **BP** or Becke−Perdew method, in which Becke's exchange functional[25] is combined with Perdew's correlation functional.[26]

2. The **B3P** hybrid method. B3P is a linear combination of various exchange and correlational functionals in the form:

$$A \cdot E_x[\text{HF}] + (1 - A) \cdot E_x[\text{S}] + B \cdot \Delta E_x[\text{B}]$$
$$+ E_c[\text{VWN}] + C \cdot \Delta E_c[\text{P86}]$$

where $E_x[\text{HF}]$, $E_x[\text{S}]$, and $\Delta E_x[\text{B}]$ are the HF, Slater, and Becke exchange functionals; and $E_c[\text{VWN}]$ and $\Delta E_c[86]$ are the Vosko, Wilk, and Nussair[27] and Perdew[26] correlation functionals, respectively. Note that $\Delta E_x[\text{B}]$ is a gradient correction to the S + WVN or LSDA for exchange, and $\Delta E_c[\text{P86}]$ is a gradient correction for correlation.

The constants A, B, and C are those determined by Becke by fitting heats of formations ($A = 0.2$, $B = 0.72$, $C = 0.81$).[28] Note that Becke used the Perdew−Wang (PW91) functional instead of P86.[28]

3. The **B3LYP** hybrid method. It is a logical extension of Becke's three-parameter concept using different correlational functionals (e.g.,

LYP) in the form:

$$A \cdot E_x[\text{HF}] + (1 - A) \cdot E_x[\text{S}] + B \cdot E_x[\text{B}]$$
$$+ (1 - C) \cdot E_c[\text{VWN}] + C \cdot E_c[\text{LYP}]$$

The constants A, B, and C are selected to be equal to those determined by Becke for the B3P method.[26]

GAUSSIAN 94[24] uses numerical quadrature to evaluate the DFT integrals. The quadrature scheme is defined by the number of points in the radial and angular directions. The geometries were optimized with a fine-pruned grid having 75 radial shells and 302 angular points per shell that resulted in about 7000 points per atom.

The HF and GGA−DFT calculations were carried out using 3−21G,[29] 6−31G(d), 6−31+G(d, p), and 6−311+G(d, p)[30] basis sets.

Energetics

RELATIVE STABILITIES

The MM2*, HF, GGA−DFT total energies (E), energy differences (ΔE), and corrected HF/ 6−31F(d) zero-point energy differences (ΔZPE) of the stable rotamers of $^1C_4$ α-L-fucose that are provided by the MM2*-SUMM search within a 40-kJ/mol energy window are summarized in Table I. The orientations of the four hydroxyl groups are notated by t, g+, or g− corresponding to the notation in Figure 1 . This provides a convenient line notation for the orientation of four hydroxyl groups.[14, 15] It should be noted that, due to the interactions, the C—C—OH dihedral angles are usually far from their idealized values (e.g., 180° for t, 60° g+). The results listed in Table I show qualitatively that the orientations of the hydroxyl groups are not independent of each other. In the most stable conformation, the number of possible OH⋯O interactions is maximal, which leads to the formation of an intramolecular chain of hydroxyl groups. The formation of these chains leads to counterclockwise or clockwise patterns as viewed from above the pyranose ring (cf. Fig. 1). The C1—O1—H group may interact with the C2—O2—H group in the clockwise direction. The C2—O2—H group may interact with the C1—O1—H group in the counterclockwise direction with the C3—O3—H group in the clockwise direction. The C3—O3—H group is in an exactly analogous situation, whereas C4—O4—H may interact with the C3—O3—H group in the counterclockwise direc-

tion or with the endocyclic oxygen in the clockwise direction. The example for the counterclockwise arrangement is the t(a) g−t t(a) conformation (first row in Table I). The example for the clockwise arrangement is the g+ (a) g+ g+ g+ (a) conformation (second row in Table I). While conformations 1, 2, and 3 shown in Table I have simple unidirected chains of OH interactions, conformations 5 and 6 have two lone pairs of OH oxygens in the middle (O2 or O3) interacting with two hydrogen atoms at both sides (non-unidirected). This concentration of interactions results in somewhat less stable rotamers of $^1C_4$ α-L-fucose.

The above-mentioned interactions dramatically reduce the number of possible rotamers and clearly show strong coupling between the hydroxyl groups. In this way, the rotational entropy of the hydroxyl groups is decreased. Similar undirected patterns were found earlier by French et al.[31] using molecular modeling techniques, by Cramer and Truhlar using AM1 and PM3 methods,[14] and by Polavarapu et al.[32] at the HF/4-31G level of theory for D-glucose.

ERROR SOURCES

Previous articles report that the PM3 method provides improved description of the intermolecular hydrogen bonding.[33,34] However, for the intramolecular OH $\cdots$ O interaction in 1,2-ethanediol, the AM1 and PM3 methods fail to supply good quality results.[35] Our results support the failure of AM1 and PM3 methods for the rotamers of $^1C_4$ α-L-fucose. The AM1 and PM3 methods are unable to provide the correct minima and energetic order. For example, rotamers 3, 4, 8, 9, and 13–17 in Table I are missing from the AM1 and PM3 conformational space and some new minima [e.g., g−(a) g−t t(a), g−(a) t t g+(a), or t(a) g−t g+(a)] appear. We checked these rotamers by the HF/3–21G method and they were not predicted to be stationary. The AM1 and PM3 methods predict rotamer 10 to be the most stable and the energetic order of the remaining conformers is completely intermingled relative to higher level methods. Similar discrepancies were experienced earlier for the hydroxyl rotamers of the α-D-glucose[14] and for the relative stability of alternative chair forms of β-D-glucose.[36]

The MM2* rotamers 13, 15, and 16, in Table I, which are not predicted to be stationary by the HF and GGA−DFT methods, converge smoothly to one of the other 14 rotamers, which are predicted to be minima (cf. Table I). Earlier results for 1,2-ethanediol[20,37] show that the so-called tGt conformation of 1,2-ethanediol, which corresponds to the t g−(a) conformation of hydroxyl groups 3 and 4 in $^1C_4$ α-L-fucose, is predicted to be in high-energy state. In this specific conformation the two hydroxyl groups are in the *anti* position and a lone pair−lone pair repulsive interaction occurs. This conformation is necessarily unstable and the higher level methods clearly support this view. The MM2* method fails to reproduce this effect correctly.

Our recent study of 1,2-ethanediol[21] also showed that the MM2* force field does not provide quantitative agreement with the higher level calculations [e.g., MP2, CCSD(t)] for the OH $\cdots$ O interactions. The HF/3−21G, 6−31G(d), and GGA−DFT results in Table I show clearly the differences between the energy ordering. The HF/3−21G method provides larger relative energies (ΔE), whereas the HF/6−31G(d) method provides smaller ΔE values for the various conformers. For these basis sets, the basis set dependence of the ΔE values at the HF level is considerable ($\sim 30\%$).

The GGA−DFT methods introduce some electron correlation effects. The BP and B3P ΔE values are frequently between the HF values: ΔE(HF/3−21G) > ΔE(BP/6−31G(d)) ≥ ΔE(HF/6−31G(d)) (cf. conformations 3, 4, 5, 6, 7, 9, and 12 in Table I). However, there are several conformations, namely 2, 8, 10, 11, 14, and 17, for which the BP method provides considerable stabilization. The common feature in these conformations is the g+(a) hydroxyl at the C4 atom. Further analysis shows that this g+(a) hydroxyl group interacts with the ring oxygen; thus, the inclusion of the electron correlation is necessary to better recover this effect. More details will be given in the following section. For all the other conformations, the HF, BP, B3P, and B3LYP/6−31G(d) results agree well with each other. For a more convenient overview, Figure 2 shows the energy differences in graphic form. The BP/6−31G(d) points shown are connected by a line. The extra stability caused by the g+ (a) position of the fourth hydroxyl group is easily seen from the Figure for the conformations, 2, 8, 10, 11, 14, and 17.

The results in Table I show considerable agreement for the relative energies calculated with various DFT methods. The largest difference is 0.6 kcal/mol, and differences below 0.1 kcal/mol are not rare (cf. conformers 3, 4, and 9 in Table I). The energetic effects of the basis set extension from

TABLE I.
Line Notations, MM2*, HF and GGA – DFT Total Energies (E), relative enrgies (ΔE), and Relative Zero-Point Energies (ΔZPE) for Stable Rotamers of $^1C_4$ α-L-Fucose Found by MM2* – SUMM Search.

No.	Torsion angles[a] 1(a)	2	3	4(a)	MM2* E^b	ΔE^c	HF/3–21G E^d	ΔE^c	HF/6–31G(d) E^d	ΔE^c	ΔZPE^c	BP/6–31G(d) E^d	ΔE^c	B3P/6–31G(d) E^d	ΔE^c	B3LYP/6–31G(d) E^d	ΔE^c
1	t	g–	t	t	–97.07	0.00	–605.12709	0.00	–608.48450	0.00	0.00	–611.94819	0.00	–613.53640	0.00	–611.94575	0.00
2	g+	g+	g+	g+	–91.78	1.26	–605.12375	2.10	–608.48144	1.92	0.00	–611.94806	0.08	–613.53559	0.51	–611.94757	0.69
3	g+	g+	g+	g+	–89.90	1.71	–605.12139	3.58	–608.48017	2.71	–0.16	–611.94427	2.47	–613.53247	2.47	–611.94283	2.52
4	t	t	t	t	–89.30	1.86	–605.11973	4.62	–608.47900	3.45	–0.31	–611.94168	4.09	–613.52998	4.03	–611.94044	4.02
5	g+	g+	g–	t	–88.50	2.05	–605.11882	5.19	–608.47852	3.75		–611.94218	3.77				
6	g+	t	t	t	–88.30	2.10	–605.11905	5.04	–608.47877	3.59		–611.94244	3.61				
7	t	g+	g–	t	–86.88	2.44	–605.11700	6.33	–608.47691	4.76		–611.94010	5.08				
8	t	g+	g+	g+	–86.01	2.65	–605.11918	4.96	–608.47848	3.78		–611.94470	2.19	–613.53211	2.69		
9	t	g+	g+	g–	–85.87	2.68	–605.11763	5.94	–608.47728	4.53		–611.94092	4.57	–613.52906	4.61		
10	t	g–	g+	g+	–81.70	3.68	–605.11949	4.77	–608.47824	3.93		–611.94438	2.40				
11	t	g–	t	g+	–81.20	3.80	–605.11757	5.97	–608.47703	4.69		–611.94287	3.34				
12	t	g–	g+	g–	–80.89	3.87	–605.11754	5.99	–608.47727	4.54		–611.94063	4.75				
13	t	g–	t	g–	–80.27	4.02	→ 1[e]										
14	g+	t	t	g+	–74.89	5.31	–605.11165	9.69	–608.47232	7.64		–611.93901	5.76				
15	g+	t	t	g–	–73.23	5.70	→ 6[e]										
16	t	t	t	g–	–73.23	5.70	→ 4[e]										
17	t	t	t	g+	–72.26	5.93	–605.10892	11.40	–608.47125	8.31		–611.93607	7.61				

[a]The hydroxyl groups are numbered according to Figure 1 and the t, g+, and g–symbols are used to notate the idealized position of the hydroxyl hydrogen. The axial position (a) is show for the first and fourth hydroxyl groups. Vertical bars denote the break of the chain. [b]Kilojoules per mole. [c]Kilocalories per mole, zero-point vibrational energies were calculated from harmonic vibrational frequencies determined at HF/6–31G(d) level and scaled by a commonly used factor of 0.89. [d]Hartree. [e]Unsuccessful attempts to find the given conformer. The number after the arrow shows the final conformation reached after the geometry optimization.

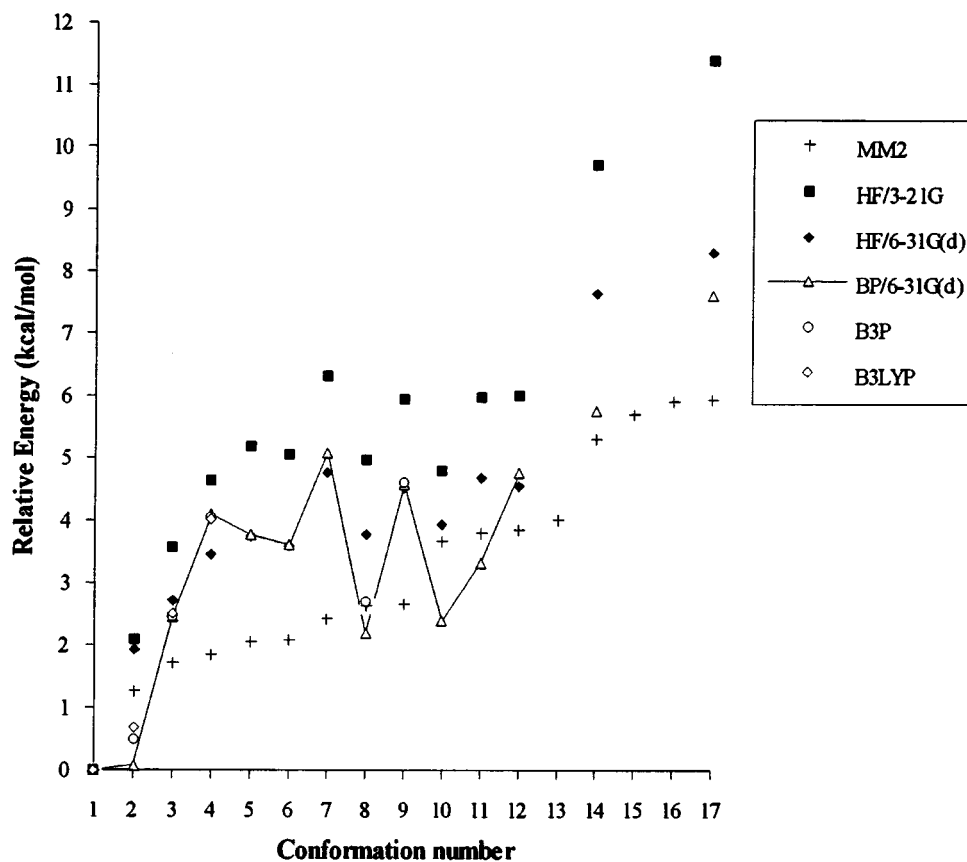**FIGURE 2.** The relative energies of $^1C_4$ α-L-fucose rotamers calculated with MM2, HF/3−21G, HF, BP, B3P, and B3LYP/6−31G(d) methods. The rotamers are numbered according to Table I.

6−31G(d) to 6−311+G(d, p) for the BP functionals are shown in Table II. These results again show considerable convergence and support use of the 6−31+G(d) basis set for GGA−DFT energetic studies as suggested by Del Bene et al.[38] The 6−31G(d) basis set can also be used with larger error bars for the energetics of rotamers; however, it should be noted that, for the energetics of the alternative chair forms, this basis set is far from being converged at the MP2 level of theory as shown by Barrows et al.[36] Our recent basis set extension study show that the GGA or hybrid DFT and MP2 methods supplements with the 6−31G(d) basis set provide similar energetic differences for the rotamers of the two chair forms of β-D-glucose and the hybrid DFT and MP2 methods agree well in regard to the energetic differences of two alternative chair forms.[39] The GGA or hybrid DFT methods supplemented with the 6−31+G(d) basis set (e.g., BP or B3P/6−31+G(d)) agree well (within 0.8 kcal/mol) with the energetic differences calculated with the MP2/cc-pTVZ methods.[39]

INTERCONVERSIONS

Figure 3 shows the possible single-step interconversions between the various rotamers of $^1C_4$ α-L-fucose. The rotamers are denoted by two numbers (the first is the MM2* and the second is the BP/6−31G(d) energetic order) in parentheses followed by a line notation. In these notations, a vertical bar (|) denotes the breaking up of a hydroxyl chain. The dual arrows connect the rotamers that differ only in one hydroxyl torsion. Because the higher level methods do not support the existence of rotamers 13, 15, and 16, they are not shown in Figure 3.

The first column of Figure 3 contains those rotamers in which all the three OH ··· OH interactions are present. As noted previously, a fourth interaction is possible as the forth g+(a) hydroxyl group interacts with the ring oxygen. The second column shows the rotamers in which exactly one OH ··· OH interaction is missing. The third column contains the rotamers in which exactly two

TABLE II.
Basis Set Dependence of Relative Energies Calculated with the BP GGA – DFT Method for the First Four Stable Rotamers of $^1C_4$ α-L-Fucose.[a]

No.	$6-31+G(d)$	$6-31+G(d, p)$	$6-311G(d)$	$6-311+G(d)$	$6-311 + G(d, p)$
1	0.00	0.00	0.00	0.00	0.00
2	1.02	1.00	0.90	1.20	0.99
3	2.60	2.52	2.67	2.63	2.42
4	3.89	3.77	4.19	3.99	3.71

[a]Energies are in kilocalories per mole. Calculations performed with BP / 6 −31G(d) geometries.

OH $\cdots$ OH interactions are missing. In this column only one rotamer can be found (17) which is the highest energy conformation according to the HF and GGA−DFT methods used in this study. All
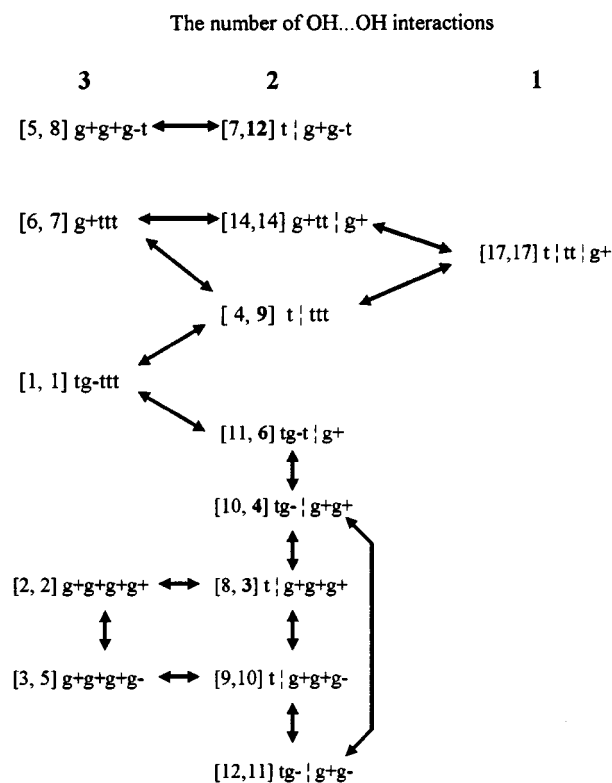
The number of OH...OH interactions

FIGURE 3. The possible single-step interconversions of the various rotamers of $^1C_4$ α-L-fucose. The rotamers are denoted by MM2* and BP/6 −31G(d) energetic order in parentheses followed by a line notation (cf. Fig. 1). If the two energetic orders differ more than four places, the BP numbers are set indicated in bold. The axial position of hydroxyl groups 1 and 4 is not explicitly shown for better readability. The dual arrows connect the conformations which differ only in one OH torsion. The breaking up of a hydroxyl chain is denoted by |. The g+ position for the fourth hydroxyl group provides an extra interaction with the ring oxygen.

other rotamers are probably not stable because, as shown earlier, the MM2* method has a tendency to provide some extra local minima; and, it probably provides an upper limit for the number of the possible rotamers. Our attempts to find further minima were unsuccessful. For example, the semiempirical results provided some new minima; we tested these rotamers at the HF level of theory and found that they are not stationary. The geometry optimizations converged smoothly to other already known rotamers. It seems that, in this respect, the semiempirical results are not reliable. We do not recommend the use of AM1 or PM3 methods for searches in the conformational space of saccharides.

Figure 3 shows that not all stable conformations are connected into a single graph by a single internal rotation. For example, conformations 5 and 7 are not connected to any other conformations. This simply means that their interconversion to another conformer requires a change in two or more hydroxyl orientations. It is believed that these interconversions are going through single-step interconversions.

BREAKING HYDROXYL CHAINS

Table III summarizes the energetic effects of breaking the OH $\cdots$ OH chains. These values can be derived for the conversions represented in Figure 3 from the differences of the corresponding ΔE values in Table I. These values are not estimates of strengths of hydrogen bonds, because the conformational energies include steric and hyperconjugative effects for $^1C_4$ α-L-fucose. Breaking the OH chain at position 1|2 in Table III is possible in two different ways. The break of the t(a) g− interaction between the first two hydroxyl groups (the 4 ⇔ 1 transition in Table III) requires about 4 kcal/mol, whereas the break of the g +(a) g + or

TABLE III.

Calculated Energy Differences (Kilocalories per Mole) Between Two Rotamers (A and B) for $^1C_4$ α-L-Fucose.[a]

Position	A ⇔ B	Methods					
		MM2*	HF/3	HF/6	BP/6	B3P/6	B3LYP/6
1|2	4 ⇔ 1	1.86	4.62	3.45	4.09	4.03	4.02
	4 ⇔ 6	−0.24	−0.42	−0.14	0.48		
	7 ⇔ 5	0.39	1.14	1.01	1.31		
	8 ⇔ 2	1.39	2.86	1.86	2.11	2.18	
	9 ⇔ 3	0.97	2.36	1.82	2.10	2.14	
	17 ⇔ 14	0.62	1.71	0.67	1.85		
3|4	11 ⇔ 1	3.80	5.97	4.69	3.34		
	14 ⇔ 6	3.21	4.65	4.05	2.15		
	17 ⇔ 4	4.07	6.78	4.86	3.52		
4(g−g+)	3 ⇔ 2	0.45	1.48	0.79	2.39	1.96	1.83
	9 ⇔ 8	0.03	0.98	0.75	2.38	1.92	
	12 ⇔ 10	0.19	1.22	0.61	2.35		

[a] The rotamers A and B are numbered according to Table I. The 3−21G basis set is symbolized by /3, and the 6−31G(d) basis set is symbolized by /6.

g+(a)t interaction (the 8 ⇔ 2 and 9 ⇔ 3 or 17 ⇔ 14 transitions in Table III) requires about 2 kcal/mol of energy at the BP/6−31G(d) level of theory.

This energetic difference might be attributed to the exo-anomeric stabilization effect.[40−45] It was supposed that, in the exo-anomeric effect, the exocyclic O1 lone pair delocalizes into the endocyclic σ*(C1—O5) bond orbital. This may occur for either the g−(a) or t(a) orientations of the anomeric hydroxyl group, whereas the g+(a) orientation does not permit exo-anomeric stabilization. Consequently, the exo-anomeric effect stabilizes conformations 8, 9, and 17, whereas it is absent from conformations 2, 3, and 14. The 4 ⇔ 1 transition is indifferent in this respect and it provides a larger energy difference. The MM2* method does not provide similar results for the exo-anomeric effect. This difference motivated us to check whether the g−(a) orientation of the first hydroxyl group would provide a new minimum at the HF/3−21G level of theory (at HF/3−21G level the exo-anomeric stabilization effect is large, cf. Table III). We started a new geometry optimization from the g−(a) g−t t(a) rotamer (it was predicted to be stable by the AM1 method). The initial geometry was constructed from the converged t(a) g−t t(a) rotamer by rotating the first hydroxyl group into the g−(a) orientation. The rotamer converged smoothly back to the t(a) g−t t(a) rotamer (row 1 in Table I) during geometry optimization. The MM2* result agrees with the HF result in this respect.

The 4 ⇔ 6 and 7 ⇔ 5 transitions in Table III provide considerably smaller energy difference. As noted earlier, the hydroxyl chains in conformations 5 and 6 are less stable (non-unidirected) and the energy gain is smaller during the formation of this type of chain. The energy requirement for breaking the hydroxyl chain between the O3 and O4 atoms is estimated to be 3.4 kcal/mol for the unidirected chains (Table III).

The stabilization effect for g+(a) position of the fourth hydroxyl can be derived from the 3 ⇔ 2, 9 ⇔ 8, and 12 ⇔ 10 in Table III. The effect is 2.4 and 2.0 kcal/mol at BP and B3P levels of theory, respectively. In the g+(a) position, the fourth hydroxyl group interacts with the lone pair of the ring oxygen. At the HF level of theory this stabilization effect is considerably smaller, being below 1.2 kcal/mol and 0.8 kcal/mol, depending on the basis set (cf. Table III).

The lower level method (MM2* and HF/3−21G) show large variations in Table III, while the GGA−DFT methods are encouragingly consistent with each other, frequently within 0.1 kcal/mol.

Structural Results

Table IV shows the structural parameters for the 14 lowest energy conformers of $^1C_4$ α-L-fucose. The numbering in Table I is used and conformations 13, 15, and 16 are excluded. In agreement

TABLE IV.
AM1, PM3, HF, and GGA – DFT Structural Parameters for 14 $^1C_4$ α-L-Fucose Rotamers.[a]

No.	Method	Bond lengths				Bond angles			Dihedral angles			
		C5—O5	C1—O5	C1—O1	C1—H	C5—O—C1	O5—C1—O1	C1—O1—H	1	2	3	4
1	AM1	1.433	1.408	1.412	1.127	115.6	106.6	107.5	182.0	−71.3	163.7	172.5
1	PM3	1.432	1.404	1.405	1.115	116.3	106.8	108.0	171.5	−66.8	160.0	176.8
1	HF/3	1.456	1.407	1.433	1.077	117.4	112.5	111.7	178.9	−79.1	163.6	168.0
1	HF/6	1.418	1.381	1.398	1.082	117.2	112.4	109.4	175.1	−78.6	165.8	169.6
1	BP/6	1.456	1.412	1.436	1.107	115.4	113.7	107.0	171.4	−78.0	159.0	161.2
1	BP/6 −sg1	1.456	1.412	1.436	1.107	115.3	113.7	107.1	171.5	−78.0	158.9	161.4
1	B3P/6	1.435	1.395	1.416	1.097	113.7	113.4	107.9	172.0	−78.3	160.4	163.0
1	B3LYP-sg1	1.444	1.402	1.425	1.097	116.1	113.2	107.8	172.9	−78.7	161.1	163.9
2	AM1	1.436	1.410	1.408	1.126	114.3	104.2	107.3	43.9	47.2	40.9	39.4
2	PM3	1.435	1.401	1.395	1.115	116.0	101.4	108.4	52.6	41.5	47.9	42.4
2	HF/3	1.458	1.421	1.420	1.077	114.2	109.7	107.8	43.6	49.9	37.6	28.5
2	HF/6	1.419	1.387	1.388	1.082	115.7	109.5	108.0	44.1	47.7	35.5	33.6
2	BP/6	1.458	1.424	1.417	1.109	113.8	110.8	104.0	31.4	42.2	42.3	37.0
2	BP/6 −sg1	1.459	1.423	1.417	1.109	113.7	110.8	104.0	30.6	42.6	42.6	37.1
2	B3P/6	1.437	1.404	1.401	1.098	114.1	110.5	105.0	34.3	43.2	41.4	35.9
2	B3LYP-sg1	1.446	1.411	1.409	1.098	114.5	110.3	105.4	35.2	44.1	41.9	36.4
3	HF/3	1.445	1.412	1.424	1.077	115.9	109.6	107.6	46.7	48.7	40.2	−65.2
3	HF/6	1.409	1.381	1.392	1.083	116.6	109.5	107.9	45.6	48.1	42.8	−69.9
3	BP/6	1.444	1.413	1.424	1.109	115.1	110.9	103.6	34.5	41.8	43.2	−73.9
3	B3P/6	1.425	1.396	1.406	1.098	115.3	110.5	104.8	37.1	43.3	42.3	−71.6
3	B3LYP-sg1	1.434	1.402	1.415	1.098	115.8	110.3	105.1	38.0	43.4	43.6	−73.0

with the experimental results,[12] the C5—O5 bond length is usually longer than the C1—O5 bond length (Table IV). The X-ray experiments indicate that the C1—O1 bond length is shorter than the C1—O5 bond length,[13, 46] and this effect is attributed to the exoanomeric effect. The calculations show that this geometric effect appears only for conformations 7 and 8 in Table IV and that it is absent from the other conformations. However, it should be noted that the comparison of the calculated and crystal structures is not straightforward because the ring hydroxyl groups orientate themselves differently in the gas phase than in the crystalline phase. In crystals, the intermolecular O⋯H interactions dominate[13, 46, 47] and the observed structures are higher energy conformers in the gas phase.[47] For the most stable conformations in the gas phase, the number of the intramolecular O⋯H interactions is maximized as it was shown previously. The method dependence of the calculated bond lengths shows that the longest bond lengths are obtained by the BP method. The HF exchange included in the B3P method provides slightly shorter C—O bonds.

The C5—O—C1 bond angle is smaller in the less stable conformations. The AM1 and PM3

methods fail to provide correct values for the O5—C1—O1 bond angle. The t position for the first hydroxyl group yields larger O5—C1—O1 and C1—O1—H bond angles than the g + position, consequently, these bond angles are coupled with the torsional angle. Comparison of C1—O—H bond angles in Table IV shows that the HF method gives bond angles that are too large. The wide C—O—H bond angle is the result of improper treatment of the electron correlation at the HF level of theory.

The hydroxyl dihedral angles frequently show large derivation (up to 30°) from the idealized values. This is a consequence of the OH⋯O interactions. The inclusion of the electron correlation turns these dihedral angles away from their idealized values to make the interactions more perfect (cf. HF and BP results in Table IV). Van den Enden et al.[48] classified the O⋯H nonbonded interactions into three major groups: π-, sp^3-, and σ-type interaction. The idealized values for the out-of-plane angle between an Ox⋯Hy vector and the Cx—Ox—H plane would be 90°, 125°, and 180°, respectively. The sp^3-type interaction seems to be energetically favorable, and hydrogen atoms are trying to maintain this angle as much as possible. For example, in the first conformer in Table IV, the

TABLE IV.
(Continued).

No. Method	Bond lengths				Bond angles			Dihedral angles			
	C5—O5	C1—O5	C1—O1	C1—H	C5—O—C1	O5—C1—O1	C1—O1—H	1	2	3	4
4 HF/3	1.457	1.417	1.419	1.080	115.9	111.8	110.9	181.7	173.9	166.9	166.2
4 HF/6	1.418	1.386	1.387	1.085	116.5	112.3	108.7	179.6	171.5	170.8	169.2
4 BP/6	1.455	1.424	1.419	1.111	114.3	113.4	106.0	180.3	165.0	159.6	160.3
4 B3P/6	1.435	1.404	1.401	1.101	114.7	113.1	106.9	179.9	166.8	162.3	162.2
4 B3LYP-sg1	1.444	1.411	1.410	1.101	115.1	113.0	106.8	180.8	169.0	163.7	163.5
5 AM1	1.433	1.406	1.411	1.126	115.0	104.3	107.0	51.0	58.1	−68.2	154.3
5 PM3								57.0	59.6	−69.3	158.6
5 HF/3	1.449	1.406	1.427	1.077	116.5	109.8	108.0	50.5	57.2	−82.2	162.1
5 HF/6	1.413	1.376	1.394	1.083	116.9	109.6	108.1	48.9	56.2	−81.6	164.9
5 BP/6	1.448	1.405	1.427	1.109	115.1	110.8	104.0	37.1	46.7	−76.6	157.9
6 HF/3	1.453	1.404	1.426	1.080	116.3	110.2	108.6	42.9	158.1	172.3	170.4
6 HF/6	1.416	1.375	1.393	1.085	116.7	109.9	108.5	41.8	156.0	174.2	172.1
6 BP/6	1.452	1.405	1.426	1.113	115.0	111.2	104.4	31.7	163.6	164.9	163.8
7 AM1	1.432	1.415	1.406	1.125	115.1	106.1	107.1	174.5	51.4	−73.4	155.4
7 PM3								160.0	56.2	−72.3	154.9
7 HF/3	1.452	1.421	1.420	1.077	115.4	110.9	111.1	174.8	52.3	−87.8	160.0
7 HF/6	1.414	1.390	1.388	1.082	116.3	111.8	108.8	174.4	56.5	−87.0	164.0
7 BP/6	1.450	1.426	1.419	1.107	113.9	112.9	106.1	176.0	50.1	−81.2	156.4
8 HF/3	1.459	1.437	1.413	1.077	113.4	111.0	111.8	169.2	41.3	37.1	31.0
8 HF/6	1.420	1.401	1.382	1.082	115.2	111.7	109.3	171.7	45.0	39.0	36.2
8 BP/6	1.459	1.445	1.411	1.107	112.8	112.7	106.7	173.5	42.4	40.3	39.9
8 B3P/6	1.438	1.423	1.395	1.097	113.3	112.4	107.6	172.4	42.3	39.7	38.6

$H2 \cdots O1$ interaction results in an $-8.5°$ deviation for the first a $-18°$ deviation for the second hydroxyl torsion resulting in $142°$ for the $H2 \cdots C1$—O1—H dihedral angle. (We prefer to use the dihedral angles instead of vector-plane angles.) In this representation, the idealized sp^3-type interaction occurs at about $105°$.[39] The same rotation turns one of the lone pairs of the second hydroxyl groups into a more advantageous position for the interaction with the H3 atom resulting in $114°$ for the $H3 \cdots C2$—O2—H dihedral angle. Further analysis of these type of dihedral angles indicates that they are between $104°$ and $140°$, depending on the positions of the interacting hydroxyl groups. The two sp^3-type regions of an oxygen atom are separated by a σ region, where the interaction is weaker. Our results obtained for 1,2-ethanediol[21] are transferable for α-L-fucose in this sense. The semiempirical methods fail to account correctly for these dihedral angles. Our analysis of the PM3 core repulsion functions (CRF) showed that there is a spurious unphysical minimum on the H—H and O—H CRF, making the

PM3 method inadequate for the present study (cf. Table IV and Ref. 49).

The GGA−DFT methods presented in Table IV account correctly for the expected correlation effects. It should be noted that the GAUSSIAN 94 implementation of the DFT method is considerably slower than the HF method with the same basis set. The large grid size used makes the calculations rather expensive. Our results in Table IV, show that, using a less dense, so-called SG1 grid (pruned to about 3000 points per atom),[24] does not deteriorate the results for the α-L-fucose, thus saving one third of the computer time.

Our detailed analysis of the dihedral angles showed that the H—Cx—Ox—H dihedral angles can be derived correctly (within 3°) from the C—Cx—Ox—H dihedral angles by subtracting 120° (if $x = 1, 2$) or adding 120° (if $x = 3, 4$) at the HF and GGA−DFT levels of theory. This provides around $+52°$ and $−90°$ for the H—C1—O2—H dihedral angle in the various conformers. No *anti* position for the H—C1—O1—H dihedral angle appears in the 14 conformations investigated here.

TABLE IV.
(Continued).

No.	Method	Bond lengths				Bond angles			Dihedral angles			
		C5—O5	C1—O5	C1—O1	C1—H	C5—O—C1	O5—C1—O1	C1—O1—H	1	2	3	4
9	HF/3	1.448	1.428	1.418	1.077	114.9	110.7	111.4	171.6	39.9	39.8	−70.2
9	HF/6	1.411	1.395	1.386	1.082	116.0	111.6	109.0	172.6	45.0	42.6	−73.0
9	BP/6	1.446	1.434	1.417	1.107	113.9	112.7	106.4	174.6	41.8	41.3	−77.5
9	B3P/6	1.426	1.414	1.400	1.097	114.3	112.3	107.3	173.4	41.8	41.3	−74.4
10	AM1	1.435	1.413	1.408	1.127	114.5	106.5	107.5	177.0	−57.2	52.1	41.0
10	PM3								167.2	−53.2	59.3	45.7
10	HF/6	1.421	1.392	1.393	1.082	115.3	111.8	109.7	171.2	−68.5	45.7	35.7
10	BP/6	1.461	1.429	1.428	1.107	112.7	112.5	107.4	170.2	−76.1	42.1	39.7
11	AM1	1.437	1.411	1.410	1.127	114.9	106.6	107.6	180.2	−69.8	167.0	53.7
11	PM3								169.7	−65.5	168.3	60.3
11	HF/3	1.467	1.420	1.427	1.078	115.3	111.8	112.0	176.3	−78.4	163.0	32.1
11	HF/6	1.426	1.389	1.394	1.082	116.1	112.1	109.7	173.3	−78.4	169.5	41.2
11	BP/6	1.468	1.426	1.429	1.107	113.8	112.9	107.4	170.0	−79.1	164.8	38.9
12	AM1	1.432	1.413	1.409	1.126	114.7	106.3	107.6	177.4	−57.5	60.9	−38.3
12	HF/3	1.447	1.413	1.431	1.077	115.7	111.4	111.7	174.3	−66.2	51.2	−73.5
12	HF/6	1.412	1.386	1.397	1.082	116.3	111.7	109.5	172.2	−67.9	52.5	−75.7
14	HF/3	1.465	1.418	1.420	1.080	114.6	109.8	108.3	35.8	153.0	175.5	27.7
14	HF/6	1.424	1.384	1.389	1.085	115.7	109.7	108.5	37.4	151.8	180.1	35.5
14	BP/6	1.463	1.421	1.417	1.112	113.5	110.8	104.3	25.2	160.6	174.3	35.3
17	HF/3	1.468	1.430	1.415	1.081	114.3	111.4	111.1	179.0	173.0	169.8	32.5
17	HF/6	1.426	1.394	1.384	1.086	115.6	112.1	108.9	178.4	170.8	176.2	41.7
17	BP/6	1.466	1.438	1.413	1.111	112.9	112.8	106.2	178.7	164.0	168.2	38.8

[a]Bond lengths in angstroms, bond angles in degrees. Conformations are numbered according to the Table I. The 3−21G basis set is symbolized by /3, the 6−31G(*d*) basis set is symbolized by /6. The GGA−DFT calculations performed with a fine grid (∼7000 points per atom), the calculations performed with the less dense grid are denoted by sg1 (∼3000 points per atom).

This supports the view that the smaller magnitude of the vicinal coupling constants of the first axial hydroxyl is the result of the *gauche* H—C—O—H dihedral angle; however, the magnitude differs considerably from the ±44° proposed Gillet et al.[16]

The larger vicinal coupling constants of the equatorial hydroxyls were attributed partially to *anti* H—C—O—H dihedral angles.[16] Analysis of the various conformations clearly shows that, for the equatorial hydroxyl groups, the *anti* H—C2—O2—H and H—C3—O3—H dihedral angles appear 4 times out of 14. This again supports, at least qualitatively, the reasoning followed by Gillet et al.[16] However, for the fourth axial hydroxyl group, the *anti* position appears 6 times out of 14. This quantitatively and qualitatively contradicts the reasoning followed by Gillet et al.[16] Solvent effects can modify these results only slightly and the interactions between the hydroxyl groups may persist in aqueous solution.[35]

Conclusions

The following conclusions can be drawn from the present investigation:

1. The MM2*-SUMM search provided 17 low-energy rotamers for $^1C_4$ α-L-fucose within a 40-kJ/mol energy window. The HF and GGA−DFT methods reduced this number to 14.
2. The orientations of the hydroxyl groups are not independent of each other. In the most stable rotamers, the number of possible OH⋯O interactions is maximal, leading to the formation of an intramolecular chain of hydroxyl groups. The formation of these chains leads to counterclockwise or clockwise unidirected, or concentrated, non-unidirected patterns. The concentration of the interac-

tions results in somewhat less stable conformations. These interactions dramatically reduce the number of possible rotamers and the rotational entropy of the hydroxyl groups. This makes sugars effective information encoders.

3. The BP, B3P, and B3LYP methods provided very similar and consistent results for the energetic order of the various rotamers for $^1C_4$ α-L-fucose. The AM1 and PM3 methods are unable to provide the correct minima and energetic order.

4. Breaking the non-unidirected concentrated OH chains requires less energy than breaking the unidirected OH chains.

5. The GGA−DFT methods correctly reflect the expected structural changes due to the inclusion of electron correlation. The so-called sp^3 type of interaction between the hydroxyl groups is energetically favorable, and the interacting hydrogen atoms attempt to maintain 105° to 120 for the Hy$\cdots$Cx—Ox—Hx dihedral angle. The deficiencies of the HF method result in the wrong C—O—H equilibrium bond and C—C—O—H dihedral angles.

6. In the proton NMR spectra of the $^1C_4$ α-L-fucose, larger vicinal H—C—O—H coupling constants were observed for the equatorial hydroxyls than for the axial hydroxyls. On this basis, it was assumed that the equatorial hydroxyls prefer the *anti* position more than the axial hydroxyl groups. Our results show that this is true for the first axial hydroxyl group and is not true for the fourth axial hydroxyl group in the gas phase.

Acknowledgments

References

1. T. H. Tang, D. M. Whitfield, S. P. Douglas, and I. G. Csizmadia, *Can. J. Chem.*, **70**, 2234 (1992).

2. X. Martin, M. Moreno, and J. M. Lunch, *Tetrahedron*, **50**, 6689 (1994).

3. M. L. Phillips, E. Nudelman, F. C. A. Gaeta, M. Perez, A. K. Shinagal, S. Hokomor, and J. C. Paulson, *Science*, **250**, 1130 (1990).

4. M. D. Lee, G. E. Ellestad, and D. B. Borders, *Acc. Chem. Res.*, **24**, 235 (1991).

5. K. C. Nicolaou, W. M. Dai, S. C. Tsay, V. A. Estevez, and W. Wrasildo, *Science*, **256**, 1172 (1992).

6. R. E. Reeves, *J. Am. Chem. Soc.*, **71**, 215 (1949).

7. M. K. Dowd, A. D. French, and P. J. Reilly, *Carbohydr. Res.*, **264** 1,(1994).

8. D. A. Cumming and J. P. Carver, *Biochemistry*, **26**, 6664 (1987).

9. J. P. Carver, S. W. Michnik, A. Imberty, and D. A. Cumming, In *Carbohydrate Recognition in Cellular Function (CIBA Foundation Symposium 158)*, Wiley, New York, 1989, p. 231.

10. J. P. Carver, *Pure Appl. Chem.*, **65**, 763 (1993).

11. J. W. Brady and R. K. Schmidt, *J. Phys. Chem.*, **97**, 958 (1993).

12. J. L. Asensio and J. Jimenez-Barbero, *Biopolymers*, **35**, 55 (1995).

13. D. Lamba, A. L. Segre, G. Fabrizi, and G. Matsuhiro, *Carbohydr. Res.*, **243**, 217 (1993), and references cited therein.

14. C. J. Cramer and D. G. Truhlar, *J. Am. Chem. Soc.*, **115**, 5745 (1993).

15. G. I. Csonka, I. Kolossváry, P. Császár, K. Eliás, and I. G. Csizmadia. *J. Mol. Struct. (THEOCHEM)*, in press.

16. B. Gillet, D. Nicole, J.-J. Delpuech, and B. Gross, *Org. Magn. Res.*, **17**, 28 (1981).

17. J. M. Goodman and W. C. Still, *J. Comput. Chem.*, **12**, 1110 (1991).

18. N. L. Allinger, *J. Am. Chem. Soc.*, **99**, 8127 (1977).

19. M. J. S. Dewar, E. G. Zoebisch, and E. F. Healy, *J. Am. Chem. Soc.*, **107**, 3902 (1985).

20. J. J. P. Stewart, *J. Comput. Chem.*, **10**, 209 (1989).

21. G. I. Csonka and I. G. Csizmadia, *Chem. Phys. Lett.*, **243**, 419 (1995), and refereences cited therein.

22. W. C. Still, MacroModel 4.5, Columbia University, New York USA.

23. (a) J. W. Ponder, F. M. Richards, *J. Comput. Chem*, **8**, 1016 (1987).
(b) T. Schlick and M. Overton, *J. Comput. Chem.*, **8**, 1025 (1987).

24. M. J. Frisch, G. W. Trucks, M. Head-Gordon, P. M. W. Gill, M. W. Wong, J. B. Foresman, B. G. Johnson, H. B. Schlegel, M. A. Robb, E. S. Replogle, R. Gomperts, J. L. Andres, K. Raghavachari, J. S. Binkley, C. Gonzalez, R. L. Martin, D. J. Fox, D. J. DeFrees, J. Baker, J. J. P. Stewart, and J. A. Pople, GAUSSIAN 94, Rev. B, Gaussian, Inc., Pittsburgh, PA, 1995.

25. J. P. Perdew, *Phys. Rev. B*, **33**, 8822 (1986).

26. A. D. Becke, *Phys. Rev. A*, **38**, 3098 (1988).

27. S. H. Vosko, L. Wilk, and M. Nussair, *Can. J. Phys.* **58**, 1200 (1980).

28. A. D. Becke, *J. Chem. Phys.* **98**, 5648 (1993).

29. J. S. Binkley, J. A. Pople, and W. J. Hehre, *J. Am. Chem. Soc.*, **102**, 939 (1980).

30. W. J. Hehre, L. Radom, P. v. R. Schleyer, and J. A. Pople, *Ab Initio Molecular Orbital Theory*, Wiley, New York, 1986, and references cited therein.

31. A. D. French, R. S. Rowland, and N. L. Allinger, In *Computer Modeling of Carbohydrate Molecules (ACS Symposium Series No. 430)*, A. D. French and J. W. Brady, Eds., American Chemical Society, Washington, DC, 1990, p. 120.

32. P. L. Polavarapu and C. S. Ewig, *J. Comput. Chem.* **13**, 1255 (1992).

33. J. J. P. Stewart, *J. Comput. Chem.*, **10**, 221 (1989).

34. M. W. Jurema and G. C. Shields, *J. Comput. Chem.* **14**, 89 (1993).

35. C. J. Cramer and D. G. Truhlar, *J. Am. Chem., Soc.*, **116**, 3892 (1994).

36. S. E. Barrows, F. J. Dulles, A. D. French, and D. G. Truhlar, *Carbohydr. Res.*, **276**, 219 (1995).

37. B. J. Treppen, M. Cao, R. F. Frey, C. Van Alsenoy, D. M. Miller, and L. Schäfer, *J. Mol. Struct. (Theochem)*, **314**, 169 (1994).

38. J. E. Del Bene, W. B. Person, and K. Szczepaniak, *J. Phys. Chem.*, **99**, 10705 (1995).

39. G. I. Csonka, K. Éliás, and I. G. Csizmadia, *Chem. Phys. Lett.* **257**, 49 (1996).

40. A. J. Kirby, The Anomeric Effect and Related Steroelectronic Effects at Oxygen, Springer-Verlag, New York, 1983.

41. R. U. Lemieux. Explorations with Sugars: How Sweet It Was, American Chemical Society, Washington, DC, 1990.

42. S. Wolfe, M.-H. Whangbo, D. J. Mitchell, *Carbohydr. Res.*, **69**, 1, (1979).

43. I. Tvaroška, and T. J. Kozár, *Am. Chem. Soc.*, **102**, 6929 (1980).

44. J.-P. Praly, R. U. Lemieux, *Can. J. Chem.*, **65**, 213 (1987).

45. I. Tvaroška, and T. Bleha, *Adv. Carbohydr. Chem. Biochem.*, **47**, 45 (1989).

46. F. Longchambon and H. Giller-Pandraud, *Acta Cryst.*, **B33**, 2094 (1977).

47. U. Salzner and P. v. R. Schleyer, *J. Org. Chem.*, **59**, 2138 (1994).

48. L. Van den Enden, C. Van Alsenoy, J. N. Scarsdale, and L. Shäfer, *J. Mol. Struct. (Theochem)*, **104**, 471 (1983).

49. G. I. Csonka, *J. Comput. Chem.*, **14**, 895 (1993), and references cited therein.